

AD-A111 739 NAVAL AIR DEVELOPMENT CENTER WARMINSTER PA SENSORS A--ETC F/6 9/1
AN IMPROVED ELECTRO-OPTICAL IMAGE QUALITY SUMMARY MEASURE.(U)
OCT 81 A H BLUMENTHAL, S B CAMPANA
NADC-81287-10

UNCLASSIFIED

OF 1
AD-3
11-10



1.0

2.8 2.5

2.2

1.1

2.0

1.8

1.25

1.4

1.6

Resolution Test Chart

12
1

REPORT NO. NADC-81283-30



AD A1111739

AN IMPROVED ELECTRO-OPTICAL IMAGE QUALITY SUMMARY MEASURE

Alan H. Blumenthal
Stephen B. Campana
Sensors and Avionics Technology Directorate
NAVAL AIR DEVELOPMENT CENTER
Warminster, Pennsylvania 18974

1 OCTOBER 1981

PHASE REPORT

TASK NO. R01112
WORK UNIT NO. GC110

Approved for Public Release; Distribution Unlimited

DTIC FILE COPY

DTIC
ELECTE
MAR 8 1982
A

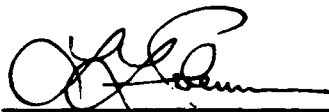
NOTICES

REPORT NUMBERING SYSTEM - The numbering of technical project reports issued by the Naval Air Development Center is arranged for specific identification purposes. Each number consists of the Center acronym, the calendar year in which the number was assigned, the sequence number of the report within the specific calendar year, and the official 2-digit correspondence code of the Command Office or the Functional Directorate responsible for the report. For example: Report No. NADC-78015-20 indicates the fifteenth Center report for the year 1978, and prepared by the Systems Directorate. The numerical codes are as follows:

CODE	OFFICE OR DIRECTORATE
00	Commander, Naval Air Development Center
01	Technical Director, Naval Air Development Center
02	Comptroller
10	Directorate Command Projects
20	Systems Directorate
30	Sensors & Avionics Technology Directorate
40	Communication & Navigation Technology Directorate
50	Software Computer Directorate
60	Aircraft & Crew Systems Technology Directorate
70	Planning Assessment Resources
80	Engineering Support Group

PRODUCT ENDORSEMENT - The discussion or instructions concerning commercial products herein do not constitute an endorsement by the Government nor do they convey or imply the license or right to use such products.

APPROVED BY:



DATE:

8 JANUARY 1982

REPORT DOCUMENTATION PAGE		READ INSTRUCTIONS BEFORE COMPLETING FORM
1. REPORT NUMBER	2. GOVT ACCESSION NO. AD-A111 739	3. RECIPIENT'S CATALOG NUMBER
4. TITLE (and Subtitle) " An Improved Electro-Optical Image Quality Summary Measure "		5. TYPE OF REPORT & PERIOD COVERED Phase
7. AUTHOR(s) Alan H. Blumenthal Stephen B. Campana		6. PERFORMING ORG. REPORT NUMBER NADC-81283-30
9. PERFORMING ORGANIZATION NAME AND ADDRESS Sensors and Avionics Technology Directorate Naval Air Development Center Warminster, PA 18974		8. CONTRACT OR GRANT NUMBER(s)
11. CONTROLLING OFFICE NAME AND ADDRESS		10. PROGRAM ELEMENT, PROJECT, TASK AREA & WORK UNIT NUMBERS Task No. Z R01112 Work Unit No. GC110
14. MONITORING AGENCY NAME & ADDRESS (if different from Controlling Office)		12. REPORT DATE 1 Oct 1981
		13. NUMBER OF PAGES
		15. SECURITY CLASS. (of this report) U
		15a. DECLASSIFICATION/DOWNGRADING SCHEDULE
16. DISTRIBUTION STATEMENT (of this Report) Unlimited distribution. Available for public release.		
17. DISTRIBUTION STATEMENT (of the abstract entered in Block 20, if different from Report)		
18. SUPPLEMENTARY NOTES		
19. KEY WORDS (Continue on reverse side if necessary and identify by block number) Johnson Criterion, Image Quality, Performance Modeling, Electro-optic Sensor Design Fiction		
20. ABSTRACT (Continue on reverse side if necessary and identify by block number) The operational performance of electro-optical imaging systems is currently predicted using models based on an approach introduced by Johnson in 1958. This model has been shown to be inadequate when used to predict performance over a wide range of conditions of signal-to-noise ratio and range to the target. This paper describes our efforts to develop and validate		

a model which is more effective than the Johnson model in predicting image quality. Implications in performance prediction modeling and electro-optic sensor design tradeoffs between sensitivity and resolution are also discussed.

AN IMPROVED ELECTRO-OPTICAL IMAGE QUALITY SUMMARY MEASURE

ALAN H. BLUMENTHAL
STEPHEN B. CAMPANA

NAVAL AIR DEVELOPMENT CENTER, WARMINSTER, PA 18974

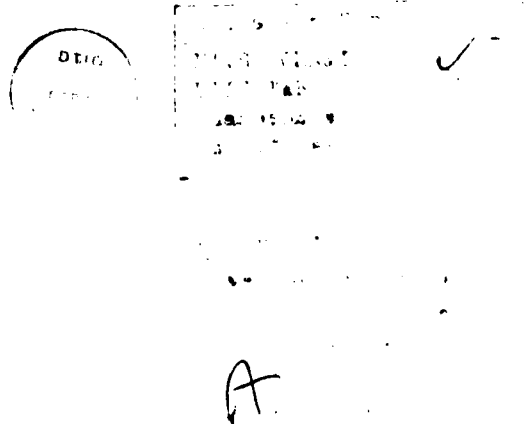
PRESENTED AT

THE 25TH ANNUAL INTERNATIONAL TECHNICAL SYMPOSIUM
OF SPIE-THE INTERNATIONAL SOCIETY FOR OPTICAL
ENGINEERING

SAN DIEGO, CA
24-28 AUG 1981

THIS WORK WAS PERFORMED UNDER
NAVAL AIR DEVELOPMENT CENTER
INDEPENDENT RESEARCH

TASK NO. R01112 WORK UNIT NO. GC110



An improved electro-optical image quality summary measure

Alan H. Blumenthal
Stephen B. Campana

Naval Air Development Center, Warminster, Pennsylvania 18974

Abstract

The operational performance of electro-optical imaging systems is currently predicted using models based on an approach introduced by Johnson in 1958. This model has been shown to be inadequate when used to predict performance over a wide range of conditions of signal-to-noise ratio and range to the target.

This paper describes our efforts to develop and validate a model which is more effective than the Johnson model in predicting image quality. Implications in performance prediction modeling and electro-optic sensor design tradeoffs between sensitivity and resolution are also discussed.

Introduction

Over the past twenty years we have seen many changes in electro-optical imaging systems. Evolutionary changes in photocathodes, television camera tubes, and infrared detectors have occurred. We have also seen revolutionary changes such as microchannel plate intensifiers, charge coupled devices, and infrared focal plane arrays. During this same period the "Johnson Criterion" has endured as the foundation for models predicting field performance of military imaging systems. However, laboratory and field experiments done in 1974 by George O'Neill¹ of the Naval Air Development Center question the accuracy of the Johnson model when applied over a wide range of video signal-to-noise ratios (SNR). Over the past several years, as our involvement with "next generation" infrared imagers has grown, we have become increasingly aware of the need for a model that better describes the quality of electronically generated images. This paper describes the progress of our effort over the past year to develop such a model.

The Johnson criterion

In 1958 Johnson² described an approach for estimating the maximum range at which a given task, e.g., detection, recognition, or identification of a target, can be done with an imaging system. This approach is based on the limiting resolution of that system as measured under the same ambient conditions encountered in the field. According to the Johnson concept, if at any given range the minimum target dimension subtends a specified number of cycles of a periodic pattern resolvable under the conditions of the test, that target could be discriminated at the corresponding level. The process of relating a test pattern to the target of interest is illustrated in figure 1. The specific number of resolvable half-cycles across the minimum dimension required to detect, recognize, or identify was determined empirically from field experiments involving such instruments as an optical telescope, image intensifiers, and an intensified image orthicon television camera, with which targets such as soldiers, artillery pieces, and army vehicles were viewed. It is reasonable to assume that these decision levels might be different for other types of targets and backgrounds. For example, the number of half-cycles required to positively identify a warship may be quite different than Johnson's value of 12.8. Also, it may be more appropriate to use a two-dimensional criterion to accommodate changes in viewing aspect. Moser³ suggested generalizing Johnson's criterion by specifying the number of square picture elements or pixels that the target area must subtend before a given task can be accomplished. The pixel size is defined by the width of a half-cycle of a bar pattern resolvable under the conditions being considered.

Beyond the question of the exact number of half-cycles or pixels needed to do a given task there is a more fundamental question: does image quality or information content correlate well with limiting resolution? Implicit in Johnson-based models is the assumption that two images of a given target are of equal utility if the number of resolution cells subtended by the target is equal. That this is sometimes not the case is illustrated in figure 2. The four images in this figure were photographed from the cathode ray tube (CRT) display of a low light level television (LLLTV) system using an intensified-silicon intensified target (I-SIT) tube chain. The two upper pictures are of a standard test chart used to measure limiting resolution. In the left-hand image, the pattern brightness is adjusted to yield the highest acuity achievable with this system in the horizontal direction: 525 +25 lines or half-cycles per picture height. The right-

hand image is produced at a pattern brightness reduced to the point where horizontal resolution is shot-noise-limited to 200 ± 25 lines per picture height. The lower pair of pictures was made using ship silhouettes of the same highlight brightness levels as in the pictures above. The scale of the silhouettes is adjusted so that the size of a resolution cell at the simulated target range is nearly the same at both brightness levels: 3.6 feet in the left-hand image; 3.1 feet in the right-hand image. According to the Johnson criterion, the right-hand image should be slightly better since more bars at the limiting resolution are subtended by the nominal ship height. Similarly, since both images are of the same broadside view of the ship, Moser's pixel criterion would favor the right-hand image slightly. Under these same conditions, NAVAIRDEVCON observers viewing the monitor and the original photographs agree that the left-hand image provides much more information about the ship.

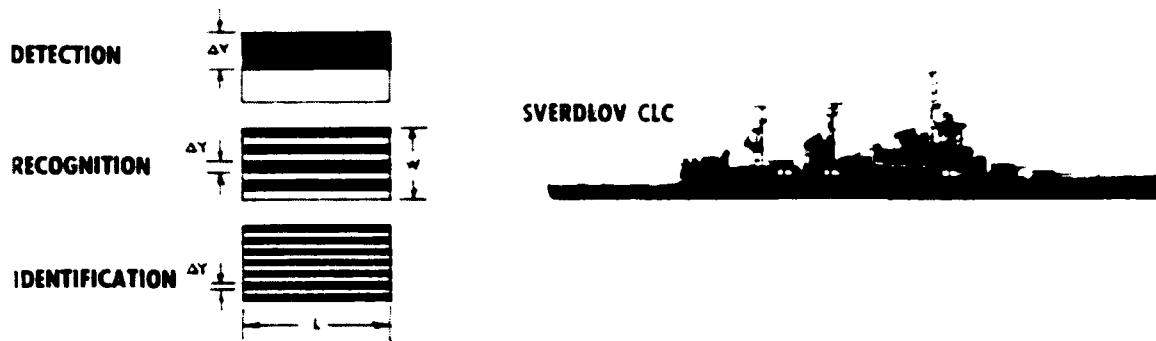


Fig 1. The Johnson criterion relates limiting resolution density to a critical target dimension

Broadband quality measures

There is a reasonable explanation for the apparent failure of the Johnson model to determine image quality over the range of conditions spanned by figure 2. In the left-hand exposure, SNR is high, and acuity is limited by the spatial frequency response of the various elements in the image producing chain. Under these conditions a series of bars blur together, so that the observer cannot distinguish or resolve them. However, most of the detail useful in distinguishing ship silhouettes is aperiodic in nature. Since the signal power contained in images of aperiodic detail such as spars or superstructure is spread across the spatial frequency spectrum, it does not suffer as greatly as the periodic bar patterns when range is increased. In the right-hand exposure it is SNR rather than spatial frequency response that limits resolution. Since the noise is broadband, it limits aperiodic signals at least as much as periodic signals.

This heuristic explanation suggests that a model which weighs signal and noise over the entire video spectrum might be more effective in determining image quality, at least for ship targets, where aperiodic detail is prevalent. This concept of a broadband frequency-weighted summary measure is, of course, not new. Biberman⁴ cites the work of Hufnagel in 1965, which offers several broadband measures for assessing the image quality of photographs. Snyder⁵ extends to electronically produced images a similar concept introduced by Charman and Olin in 1965, and demonstrates correlation between the resulting measure and observer performance with raster-scan images. The focus of our work over the past year was to develop these and other broadband quality measures, and to compare their effectiveness in predicting relative image quality to each other and to the Johnson model.

Approach

Briefly, our approach for establishing a model that adequately predicts relative quality was to generate a series of images over a wide range of video SNR, sensor modulation transfer function (MTF), and target scale. The images were generated by photographing the display of a vidicon camera system viewing silhouettes of the broadside view of a Soviet KOTLIN class destroyer. Observers were then asked to rank order the images according to the amount of information they could glean from each exposure. This rank ordering was then correlated to the orderings dictated by several candidate figures of merit, including the Johnson criterion. The degree of correlation and the lack of many obvious mismatches or "wild points" in the correlation plot provides an indication of the effectiveness of a given figure of merit. Following is a more detailed account of the image generation process and of the technique for establishing observer ranking.

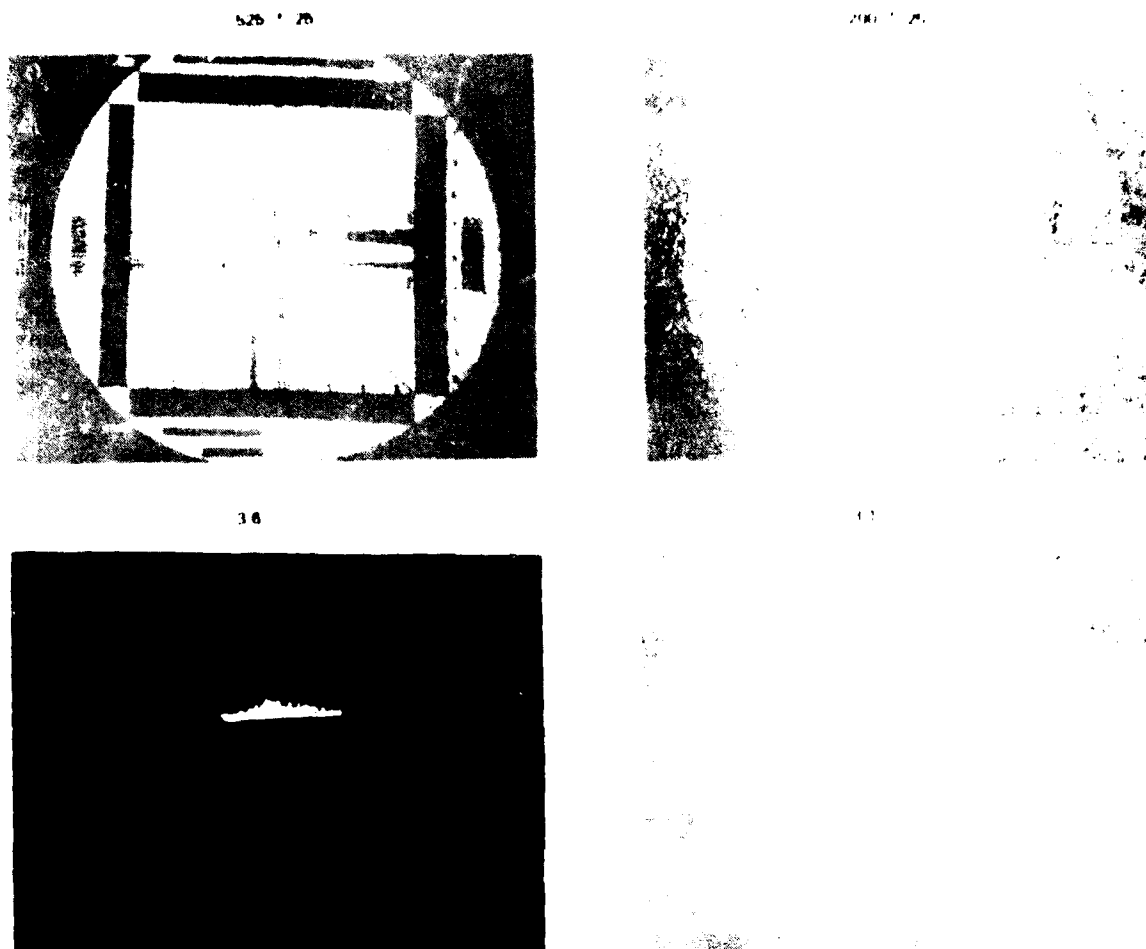


Fig 2. Comparison of video imagery at high (left) and low (right) signal-to-noise ratio

Image generation

Figure 3 is a block diagram of the facility used to generate the series of hard copy images. Transparencies of the broadside KOTLIN silhouette were made with the scale factor ranging from 136 to 1810 meters per picture height. These transparencies were back illuminated in a 610-mm focal length collimator, with a well-regulated incandescent lamp. An antimony trisulfide vidicon camera with a 75 mm focal length lens was aligned with the collimator to produce the electronic image of the ship. The 525-line, 30-frame-per-second video signal and white noise were added and passed through an 8-MHz lowpass filter. Signal and noise levels were controlled independently to achieve the desired SNR, while at the same time filling the brightness range of the display without clipping of the noise. This condition was insured through an elaborate procedure using an electronically generated gray scale and a photometer to measure the resultant display brightness. Video signal was determined by digitally measuring the mean difference between the voltage at points within the silhouette and the voltage in the darker background. The root-mean-square (RMS) noise was determined by measuring the frame-to-frame variance of the voltage at a point in or around the silhouette. SNR is defined herein as the ratio of the difference signal to the RMS noise.

The spatial frequency response, expressed in terms of the MTF was controlled by defocussing the television camera lens. MTF was measured using the same minicomputer-based system used to determine signal and noise. Schade's¹ noise-equivalent passband, N_o , was used to describe MTF with a single number. N_o is defined as:

$$N_e = \int_0^{\infty} (MTF(f))^2 df. \quad (1)$$

For this experiment two values of N_e were used: 45 and 185 lines per picture height.

Each image was photographed from a 21-inch CRT with a 35 mm single lens reflex camera. Kodak Plus-X film was used for the black and white prints; Ektachrome 200 with color-correcting filters was used to make 35 mm slides. Trial exposures showed that the light and dark banding produced by the temporal and spatial relationship between the camera focal plane shutter and the TV raster scanning would be objectionable. This banding was avoided by blanking the video so that while the shutter was open the monitor displayed exactly three frames of video. The 0.1-second exposure time was chosen to simulate the noise equivalent integration time of the typical human observer viewing a display of about 30 footlamberts.

Eight values of SNR, 6 scale factors, and 2 N_e factors were used to make up the total of 96 different images generated. These values were: 0.3, 0.5, 1.0, 2.0, 4.0, 8.0, 12.0, and 100.0 for SNR; 136, 197, 388, 543, 724, and 1810 meters per picture height for the scale factor; and 45 and 185 TV lines per picture height for N_e . Figure 4 is a composite of the 48 images produced for $N_e = 185$.

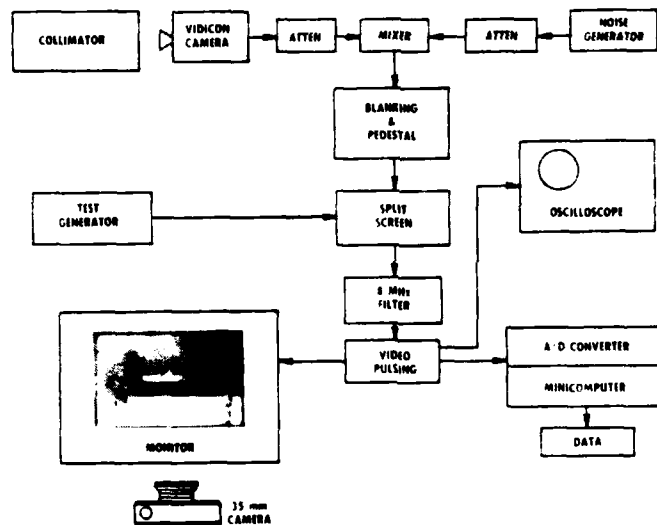
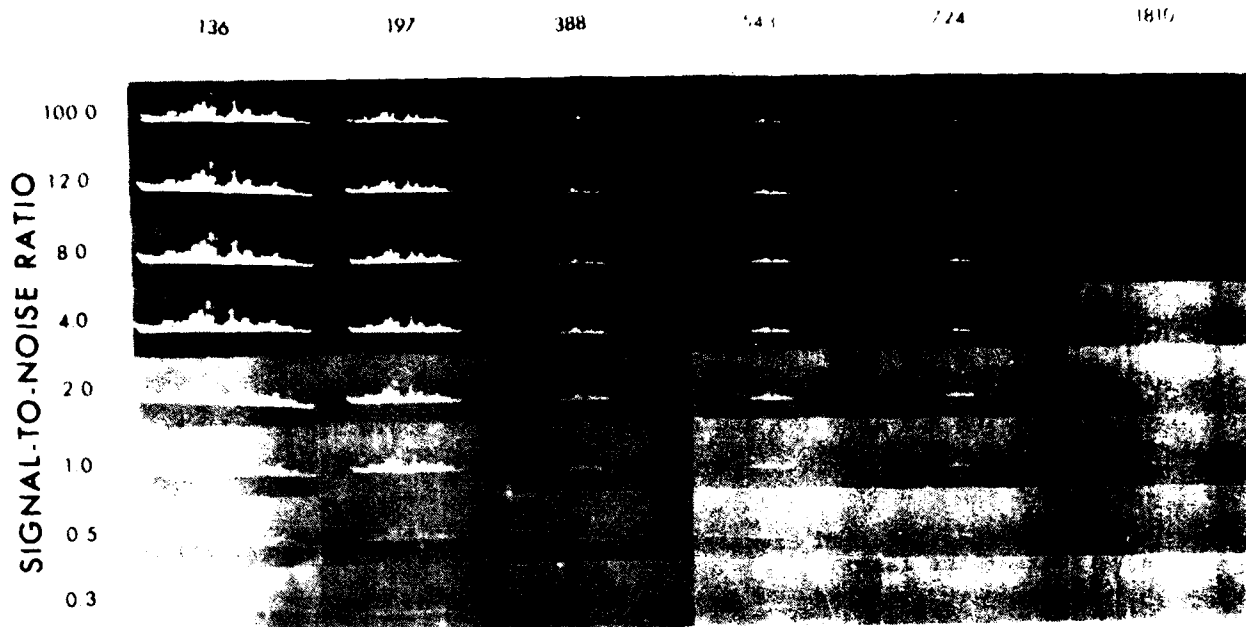


Fig 3. Block diagram of the equipment used to generate test images

Image ranking

A group of engineers and physicists was used to establish subjective rank ordering of the 96 images. All had vision corrected to 20/20; none was specifically trained in ship identification. Prior to the rank ordering process, each observer was shown a print of the highest quality image of the ship, and was instructed to note the position and appearance of guns, masts, and superstructure. He/she was then shown pairs of images projected by two slide projectors, with brightness carefully matched and maintained. The distance between the observers and the screen was maintained at twice the height of the projected slide. He/she was given unlimited time to decide which of the two slides conveyed more information about the ship. Sequencing of the pairs was governed by the observer's response, using a procedure that avoided showing pairs with obviously disparate image quality. In this manner, all significant comparisons were completed in less than 3-hours of total viewing time, broken up into three sessions on 2 days, with 15-minute breaks after 20 minutes of viewing. At the end of the procedure the observer was shown the slides in the order that his/her responses dictated, and was given the opportunity to reverse the decision on close calls. Orderings were determined for nine different people. Ranking was also done by several observers using 5-in. x 7-in. black and white prints. These orderings proved consistent with those done using slides.

RANGE (METERS/PICTURE HT)

Fig 4. Test images for $N_s = 185$ Results

The rankings determined by the observers were correlated with the rankings determined by 13 different figures of merit formulations. The formulations that produced the best correlations are described below:

Figures of merit

Following the work of Snyder, we evaluated an image quality model termed Modulation Transfer Function Area defined as the area between the $MTF(f)$ curve and the observer demand function, $D(f)$. This model, referred to as Q_1 has the form:

$$Q_1 = \int_0^{f_L} (MTF(f) - D(f)) df, \quad (2)$$

where f_L is the intersection of the two functions as shown in figure 5.

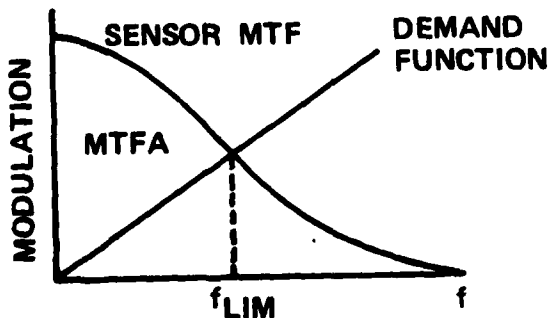


Figure 5. Parameters used for image quality models

The demand function is defined as the modulation required to resolve a periodic pattern at a given frequency, f , given the video SNR. Using the results of Coltman and Anderson, it can be shown that over a broad range of SNR

$$D(f) = f / (K \cdot \text{SNR}), \quad (3)$$

where K is a constant dependent on system parameters. For our 8-MHz bandwidth and 4:3 picture length to width ratio.

$$K = \frac{1000 \text{ lines per picture height}}{\text{height}} \quad (4)$$

As stated in equation (1), Q_1 would have the units of lines per picture height. This is referred to target space by dividing by the scale factor, H , with units of meters per

picture height:

$$Q'_1 = Q_1/H \text{ (lines/meter)} \quad (5)$$

A second model that was evaluated, termed Modulation Transfer Function Power Q_2 , is based on the integrated signal power divided by the integrated noise power:

$$Q_2 = \frac{\int_0^\infty S^2(f) (MTF)^2(f) df}{\int_0^\infty N^2(f) df} \quad (6)$$

Assuming both the signal and noise spectra are uniform, (5) can be reduced to the form

$$Q_2 = \text{SNR}^2 \int_0^\infty (MTF)^2(f) df. \quad (7)$$

Substituting equation (1) into (7) and normalizing by the scale factor yields:

$$Q'_2 = \frac{(\text{SNR})^2 N_e}{H} \quad (8)$$

A third model, termed Signal-to-Noise Ratio Threshold (SNRT), referred to as Q'_3 , is a variant of the last:

$$Q'_3 = \frac{\text{SNR}}{\text{SNR} + \text{SNR}_0} \frac{N_e}{H} \quad (9)$$

where SNR_0 is a threshold value, empirically determined to yield the highest correlation rankings. This figure of merit herein will be referred to as SNRT.

In addition to these models and many variations thereof, the Johnson-based formulation was also evaluated. Since according to Johnson, limiting resolution at the target plane is sufficient to define quality, this model termed Q'_4 is simply expressed:

$$Q'_4 = f_L/H \quad (10)$$

In our investigations limiting resolution, f_L , was calculated using the demand function and MTF as illustrated in figure 5.

Correlation of rankings

The effectiveness of a given model in predicting image quality can be gauged by comparing the rank ordering as determined with the model and the ordering determined by observation. Two approaches for comparing these orderings were used. The first was to plot the figure of merit calculated for the image placed by an observer in a given position against the figure of merit of the image that would have been in that position if the model were correct. For example, if the picture that was tenth best in an observer's estimation had a calculated figure of merit of, say A, but the picture judged by the model to be tenth best had a figure of merit equal to B, this data point would be represented by (A, B). In this manner, the cross correlation of a given observer's responses to a given model's prediction was determined for all of the observers, and for many variations of the models previously described.

The correlation coefficient proved to be a very insensitive measure of agreement. In no case was the coefficient less than 0.9. The Johnson criterion yielded values ranging from 0.943 to 0.973, depending on the observer. Figure 6a is the cross plot of the Johnson ranking with that of a typical observer. The SNRT model defined by equation (9) with the threshold constant set equal to 3.0 yielded the highest coefficients, ranging from 0.987 to 0.993. Figure 6b is the plot of this model against the responses of the same observer as in 6a. These same correlations were also done on a logarithmic scale, so that a change in quality at the low end of the scale is given equal weight as a proportional change at the high end. Coefficients were typically 5% lower than those calculated on the linear scale. Figures 7a and 7b are the logarithmic plots of the results with the Johnson and SNRT models corresponding to those in figure 6.

The second approach used to evaluate the effectiveness of a model in predicting observer response was to consider the number of points which fall far from the prediction line in any given model. Comparing figure 6a with 6b, and 7a with 7b, it appears that despite the relatively high correlation coefficient, the Johnson model is capable of

making much larger errors in estimating image quality. In table I, 12 notable "wild points" are analyzed. For each of the 12 points, the rank assigned to our "typical" observer is compared with that determined from the Johnson and SNRT models. Also given are the corresponding sensor parameters. Note that the Johnson model tends to underestimate the quality of images with high SNR values while overestimating the quality of those with low SNR. SNRT, while not perfect, yields much better agreement, and does not consistently favor high or low SNR images.

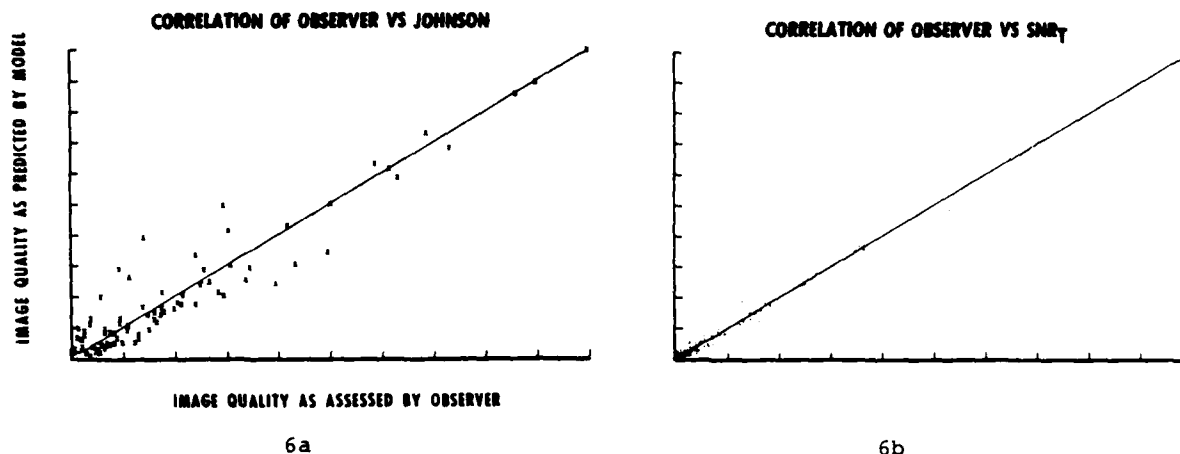


Fig 6. Correlation of image quality as assessed by observers and predicted by models
Linear scale

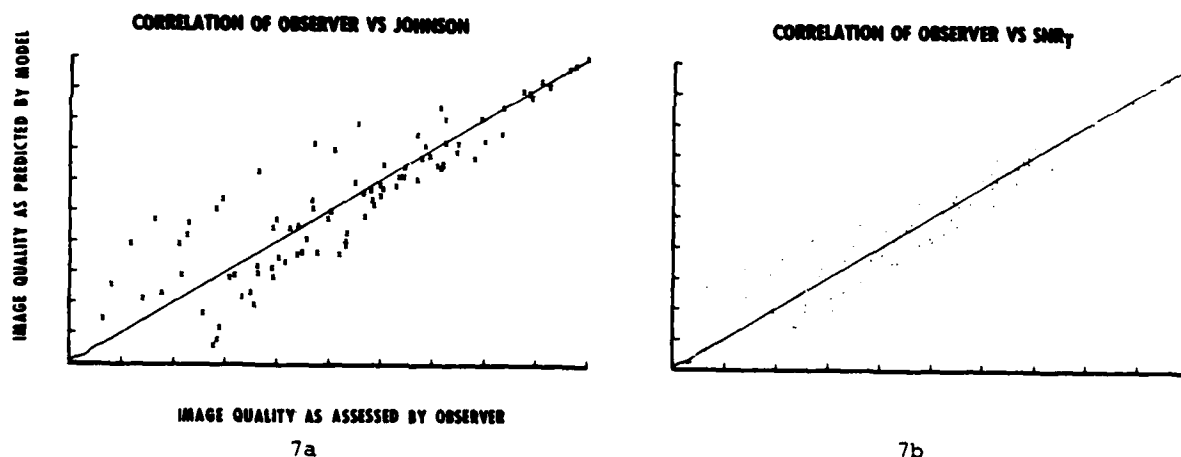


Fig 7. Correlation of image quality as assessed by observer and predicted by models
Log scale

Table I. Analysis of "Wild Points"

Observer	Rankings			Parameters	
	Johnson	SNRT	SNR	Scale (M/PH)	N_e (L/PH)
24	33	26	4.0	543	185
25	15	24	1.0	197	185
40	13	29	1.0	136	185
46	21	35	0.5	197	185
49	64	44	12.0	1810	185
50	19	39	0.3	136	185
64	30	50	0.3	197	185
74	91	81	8.0	1810	45
76	92	86	4.0	1810	45
79	58	82	0.3	197	45
84	51	67	0.3	388	45
86	61	72	0.3	543	185

Model evaluation

To evaluate further the effectiveness of the most promising of the candidate models - SNRT - vis-a-vis the Johnson approach, several additional sets of images were produced. Each set is comprised of ship images at three different ranges. The SNR of each image is adjusted so that all three images have the same quality as defined by either of the two models. These images can then be examined side by side to see which model is more effective in defining quality. Three levels of task difficulty - detection, recognition, and identification - were treated in this manner. These levels were established by asking observers to look through the ordered series of 96 photographs to determine the points at which (a) something is barely detectable, (b) the object is recognizable as a warship rather than a merchant ship, and (c) the warship is identifiable as being of the KOTLIN class. Obviously, since only KOTLIN images were used, these discrimination levels were defined only in a very relative sense, and are not meant to represent an absolute criterion.

The recognition case images are reproduced in figure 8 as a representative example of the results of this exercise. Images in the upper row are those identified by the Johnson model as being of equal quality. Images in the lower row are of equal quality as defined by the SNRT model. As the correlation exercise described previously suggests, the SNRT model is more effective in trading off SNR for target size. Figure 8 shows graphically how the Johnson model overestimates the utility of low SNR imagery, while underestimating that of high SNR.

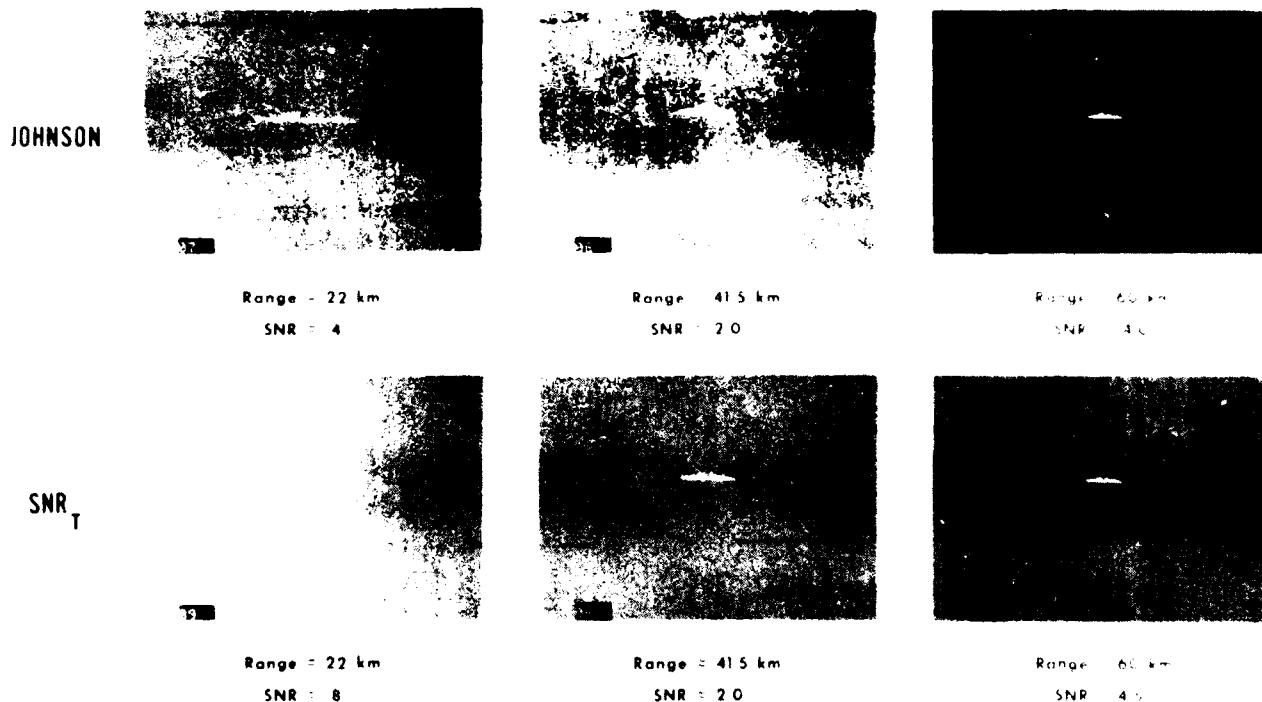


Fig 8. Images of equal quality as assessed by the Johnson and SNRT models

The SNRT model was also more successful at defining consistent detection and identification grade imagery than was the Johnson approach. These results, and the results of the correlation exercise described previously, lead us to believe that the SNRT model is more accurate in predicting image utility than is the Johnson model. In the next section, the practical impact of this conclusion on system modeling and design tradeoffs will be examined.

Implications

The experimental results described above point to a change in sensor modeling that will impact: (a) the prediction of field performance of a given system and (b) the tradeoffs made during the design of the system.

Impact on performance prediction

To explore the impact of the use of SNRT on performance modeling, we have defined a hypothetical thermal imaging system which has the same MTF as the camera used in our experiment ($N_e = 185 \text{ TVL/PH}$). Assuming the task is recognition as defined in the same sense as previously described, the Johnson and SNRT models produce the two SNR versus range curves plotted in figure 9. The five negatively sloping curves describe the SNR generated in the sensor by the thermal signature of a warship after propagation through a slant path from the surface to the sensor altitude. Range is normalized by the sensor vertical field of view. The extinction coefficients were calculated for a particular spectral band, sensor altitude, geographic location, and sensor. The curves represent conditions of SNR that would be exceeded 10, 20, 50, 80, and 90% of the time, respectively. The zero range SNR is the ratio of the target thermal contrast to the system noise equivalent thermal contrast. The intersections of either of the system demand functions with the target strength functions occur at the recognition ranges that would be exceeded 10, 20, 50, 80, or 90% of the time. Under the 10 percentile condition, the SNRT model predicts a recognition range 35% longer than the Johnson model. Under the more typical 50 percentile condition, an increase of 26% is predicted by SNRT. Repeating the exercise for the detection case produced even more significant differences in the predicted ranges. Under median weather conditions, the SNRT model predicts a detection range 43% higher than the Johnson model. In extremely good weather the discrepancy increases to over 60%.

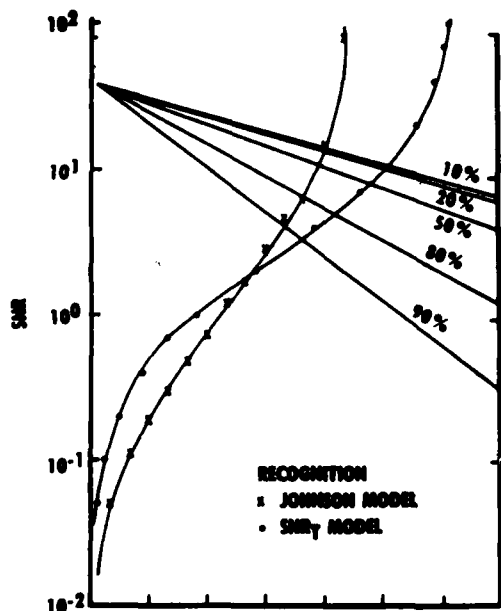


Fig 9. Comparison of performance predictions

In locations at lower altitudes where transmission is poorer, the SNRT model predicts ranges shorter than those generated by the Johnson model. Thus, depending on the environment, target, task, and system, the Johnson model can produce significant range errors in either direction.

Impact on sensor design

The Johnson model tends to underestimate the degree of system performance increase to be gained through improvement in system sensitivity. This is illustrated in figure 10, again using our hypothetical forward looking infrared (FLIR) for warship recognition. Figure 10a gives system demand functions based on the Johnson model, using two different values of system noise. The upper curve represents a system with sensitivity commensurate with what might be achieved with current detector technology; the lower curve represents a 4:1 increase in sensitivity, such as might be achievable using more detectors. The target strength curves are plotted as in the previous example. Note that according to this model the 4:1 sensitivity improvement results in a range increase of only 11% for the 50 percentile condition.

Figure 10b shows the same analysis using the SNRT model. Here the range increase is a more substantial 25%. As was the case in the previous example, the discrepancy between the Johnson model and SNRT is greater for the detection task, and less for the identification task. The relative insensitivity of the Johnson model to SNR improvement unduly biases design tradeoffs in favor of resolution, and results in systems which are less than optimum in terms of effectiveness.

Summary

Through a series of ship images produced over a wide range of SNR, MTF, and range, we have shown that the Johnson criterion tends to overestimate the utility of images made at low SNR, while underestimating the quality of high SNR images. This results in range predictions which tend to be pessimistic in situations involving strong target signatures, sensitive sensors, favorable weather, or lower order tasks, and optimistic in situations at the other extreme.

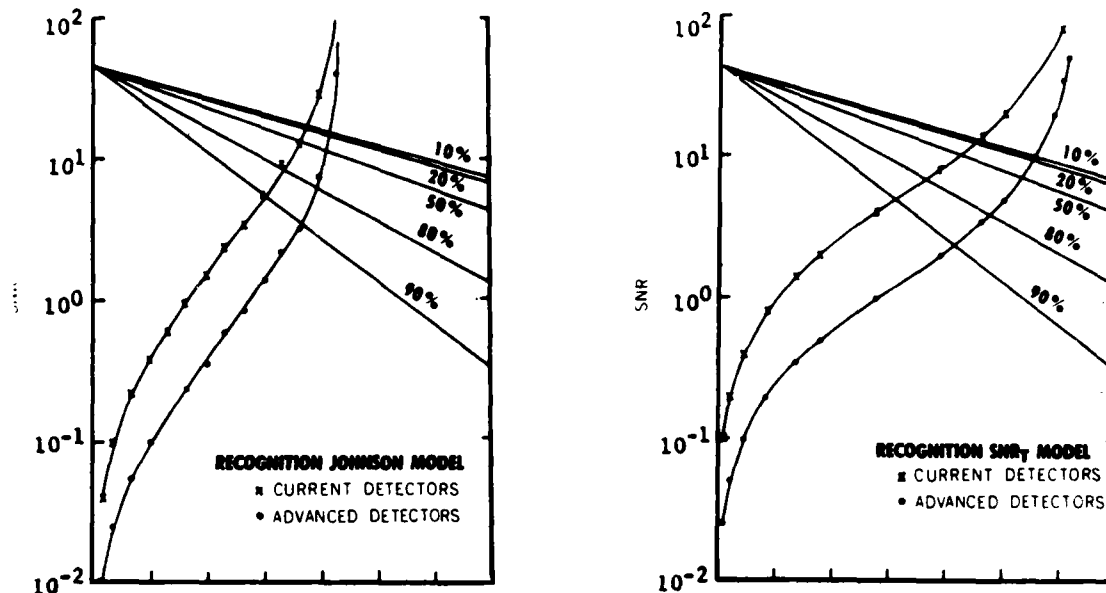


Fig 10. Comparison of performance predictions for current generation sensor and increased sensitivity sensor for the Johnson and SNRT models

We have developed a formulation which yields a higher correlation between predicted image quality and the quality as assessed by a group of observers than does the Johnson approach. This relatively simple model drives sensor design tradeoffs more in the direction of sensitivity, and is more effective in accurately predicting effective stand-off range over a broad range of conditions.

Acknowledgement

The advice and assistance of Mr. Colin Monro throughout this study is gratefully acknowledged. The authors also wish to express their gratitude to Mr. David Schuck for his help in processing data, to Mr. Roy Radzai and the members of the Photography Branch for their help in obtaining the test images, and to our panel of observers for their patience in ranking the images.

References

1. O'Neill, G., NAVAIRDEVCON Tech Memo NADC-202139 of Jan 1974
2. Johnson, J., "Analysis of Image Forming Systems" Proceedings of the US Army Engineer Research and Development Laboratories, Fort Belvoir, VA, Image Intensifier Symposium, 6-7 Oct 1958. (AD-220 160)
3. Moser, P. M., NAVAIRDEVCON Tech Memo NADC-20203A:PMM "Mathematical Model of FLIR Performance" of 19 Oct 1972 (AD-A045 247)
4. Biberman, L. M., Perception of Displayed Information, Plenum Press, New York, NY, 1973, Chapter 2
5. Snyder, H. L., Ibid Chapter 3
6. Schade, O. H., Ibid Chapter 6
7. Coltman, J. W., and Anderson, A.E., "Noise Limitations to Resolving Power in Electronic Imaging," Proceedings of the Institute of Radio Engineers 48, 5, 1950, pp 858-865.

NADC-81283-30

<u>Name</u>	<u>Code</u>	<u>Organization</u>
Nakhleh, Jamil (Dr.)	OP-03EG	CNA
Emerson, D. F. (VADM)	OP-098	CNO
Hyaward, T. B. (ADM)	OP-00	CNO
Triggs, L. E.	OP-35E	CNO
Eckstein, R. W. Jr.	802	NAC
Knight, R. D.	931	NAC
Beggs, E. B.	360	NAVAIR
Savoca, G. J.	549	NAVAIR
Hooper, E. T.	370D	NAVAIR
Klein, L. E.	549331	NAVAIR
Quinn, P. W. III	370F	NAVAIR
King, W.	360J	
Willis, J. W.	310B	NAVAIR
Thyberg, R.	03P2	
Ricketts, J. C.	310	NAVELEX
Ritter, A. D.	PME 107-52	NAVELEX
Sharn, C. F. (Dr.)	003	E-O R&T
Fletcher, P. C. (Dr.)	015	NOSC
Morreal, J. A.	7313	NOSC
Weinreich, W. C.	7313	NOSC
Whitman, W. H.	7313	NOSC
Curley, S. R.		NPGS
Sternberg, R. L.		NPGS
White, M. B.		NPGS
Barbe, D. F.		ASN (RE&S)
Bartoe, J. D. F. (Dr.)	4162	NRL
Goodell, W. V. (Dr.)	6552	NRL
Kershenstein, J. C. (Dr.)	6009	NRL
Milton, A. F. (Dr.)	6550	NRL
Steinberg, R. (Dr.)	6509	NRL
Gann, J. D.	2833	NSRDC
Ely, R. I.	F-14	NSWC/DL
Fontenot, L. J.	N-54	NSWC/DL
Bis, R. F. (Dr.)	R-33	NSWC/WOL
Goo, G.	R-42	NSWC/WOL
Katz, B. S. (Dr.)	R-42	
Marcell, F. C. (LCDR)	R-4201	NSWC/WOL
Petropolous, S. K.	R-42	NSWC/WOL
Burns, J.	214	NTEC
Mohon, N.	731	NTEC
Ankeney, D. P.	3353	NWC
Bailey, T.	3924	NWC
Benton, E. E. (Dr.)	39401	NWC
Christensen, D. L.	3942	NWC
Decker, P. R.	3107	NWC
Dodge, C.	39403	NWC
Gorrano, B. J.	31507	NWC
Holden, B. J.	3134	NWC
Saitz, D. L.	3381	NWC
Pilloff, H. (Dr.)	421	ONR

NADC-81283-30

<u>Name</u>	<u>Code</u>	<u>Organization</u>
Weinberg, E. (Dr.)	400	ONR
Lawson, R. F.		ONR-Branch
		Office
		Pasadena, CA
White, M. B. (Dr.)		ONR-Branch
		Office
		New Yor, NY
Matthews, G. B.	1232	PMTc
Townsend, C. L.	1232	PMTc
Hutcheson, E. (Dr.)	DELNV-IRTD	NV&EOL
Urban, G. D.	AFAL/RWI	AFAL
Thomas, C. (Dr.)		DARPA
Tegnelia, J. (Dr.)		DARPA
Holzer, W.		IDA
Biberman, L.		IDA
Martil, W. L.	AF AMRL/HEA	Wright-Pat AFB
Bosserman, D.	DELNV-SI	NV&EOL
Hubbard, R.	AFAL/RWU	Wright-Pat AFB
Ratches, J. (Dr.)	DELNV-V1	NV&EOL
Summers, D. E.	AAA-3	AFAL-Wright-Pat AFB
Grandjean, A.	AFAL/RW1	AFAL-Wright-Pat AFB
Schnitzler, A. (Dr.)	6550	NRL
Grant, W.	DELNV-FIR	NV&EOL
Novak, S.	DSDAR-SCF-IE	AARADCOM, DOVER,
		NJ
Peacock, D.	AFAL/DHO-3	AFAL
Deangelo, J. (Dr.)	RADC/ESRH	Hanscom AFB
	(Stop 30)	
Wunderlich, J. (Dr.)	39403	NWC
Vroombout, L.	AARI	AFAL

DATE
FILMED
-8